

Spatial scaling properties of coral reef benthic communities

Ford, Helen; Gove, Jamison M. ; Davies, Andrew; Graham, Nicholas A.J.; Healey, John; Conklin, Eric; Williams, Gareth J.

Ecography

Accepted/In press: 28/09/2020

Peer reviewed version

[Cyswllt i'r cyhoeddiad / Link to publication](#)

Dyfyniad o'r fersiwn a gyhoeddwyd / Citation for published version (APA):

Ford, H., Gove, J. M., Davies, A., Graham, N. A. J., Healey, J., Conklin, E., & Williams, G. J. (Accepted/In press). Spatial scaling properties of coral reef benthic communities. *Ecography*.

Hawliau Cyffredinol / General rights

Copyright and moral rights for the publications made accessible in the public portal are retained by the authors and/or other copyright owners and it is a condition of accessing publications that users recognise and abide by the legal requirements associated with these rights.

- Users may download and print one copy of any publication from the public portal for the purpose of private study or research.
- You may not further distribute the material or use it for any profit-making activity or commercial gain
- You may freely distribute the URL identifying the publication in the public portal ?

Take down policy

If you believe that this document breaches copyright please contact us providing details, and we will remove access to the work immediately and investigate your claim.

1 **Spatial scaling properties of coral reef benthic communities**

2

3 Helen V. Ford^{1*}, Jamison M. Gove², Andrew J. Davies³, Nicholas A. J. Graham⁴, John R.
4 Healey⁵, Eric J. Conklin⁶, and Gareth J. Williams^{1*}

5

6 ¹School of Ocean Sciences, Bangor University, Anglesey, LL59 5AB, UK

7 ²NOAA Pacific Islands Fisheries Science Centre, Honolulu, HI, USA

8 ³Department of Biological Sciences, University of Rhode Island, Kingston, RI, USA

9 ⁴Lancaster Environment Centre, Lancaster University, UK

10 ⁵School of Natural Sciences, Bangor University, Bangor, Gwynedd, LL57 2UW, UK

11 ⁶The Nature Conservancy, 923 Nuuanu Avenue, Honolulu, HI, USA

12 *Email: helen.ford@bangor.ac.uk, g.j.williams@bangor.ac.uk, Tel: +44(0)1248 382588

13

14 **Keywords:** autocorrelation, benthic ecology, physical drivers, scale, seascape, coral
15 morphology

16

17 **Abstract:**

18 The spatial structure of ecological communities on tropical coral reefs across
19 seascapes and geographies have historically been poorly understood. Here we addressed this
20 for the first time using spatially expansive and thematically resolved benthic community data
21 collected around five uninhabited central Pacific oceanic islands, spanning 6° latitude and 17°
22 longitude. Using towed-diver digital image surveys over ~140 linear km of shallow (8 – 20 m
23 depth) tropical reef, we highlight the autocorrelated nature of coral reef seascapes. Benthic
24 functional groups and hard coral morphologies displayed significant spatial clustering
25 (positive autocorrelation) up to kilometre-scales around all islands, in some instances
26 dominating entire sections of coastline. The scale and strength of these autocorrelation

27 patterns showed nuances across geographies, but patterns were more similar between islands
28 in closer proximity and of a similar size. For example, crustose coralline algae (CCA) were
29 clustered up to scales of 0.3 km at neighbouring Howland and Baker Islands and macroalgae
30 were spatially clustered at scales up to ~3 km at both neighbouring Kingman Reef and
31 Palmyra Atoll. Of all the functional groups, macroalgae had the highest levels of spatial
32 clustering across geographies at the finest resolution of our data (100 m). There were several
33 cases where the upper scale at which benthic community members showed evidence of
34 spatial clustering correlated highly with the upper scales at which concurrent gradients in
35 physical environmental drivers were spatially clustered. These correlations were stronger for
36 surface wave energy than subsurface temperature (regardless of benthic group) and turf algae
37 and CCA had the closest alignments in scale with wave energy across functional groups and
38 geographies. Our findings suggest such physical drivers not only limit or promote the
39 abundance of various benthic competitors on coral reefs, but also play a key role in governing
40 their spatial scaling properties across the seascape.

41

42 **Introduction**

43 Patterns in nature are often highly scale dependent (Levin 1992). Conclusions drawn
44 from observations at one scale may be inconsistent when observing at another scale. Scales of
45 observation in ecology are often chosen for arbitrary, logistical or anthropocentric reasons
46 and may not be appropriate for the target organism, system or process in question (Addicott
47 et al. 1987, Wiens and Milne 1989, Boström et al. 2011). Such mismatches of scale can
48 reduce our predictive capacity of ecosystem dynamics and lead to erroneous extrapolations
49 over larger scales from spatially or temporally limited sampling observations (Hatcher et al.
50 1987, Schneider 2001). Despite this, observational scales in ecology have generally remained
51 constrained and limit our understanding of the scaling of natural systems (Estes et al. 2018).

52 By conducting ecological investigations at systematically varied scales, the dynamics of
53 natural systems and how they vary as a function of scale can be properly quantified (Rahbek
54 and Graves 2000, Nash et al. 2014).

55 Since the 1980's, ecology has benefitted from an advancement of concepts related to
56 ecological pattern and scale, including the idea that biological spatial patterns emerge at
57 characteristic scales in response to their environment (Wiens and Milne 1989, Levin 1992,
58 Schneider 1994). The progression of 'landscape ecology' theory occurred alongside an
59 increased diversity of field techniques, most notably remote sensing technology (Dungan et
60 al. 2002, Wagner and Fortin 2005). These technologies greatly expanded scales of
61 observation and enabled practical implications of landscape ecology to be used in ecosystem
62 management (Lee et al. 2008, De Knegt et al. 2011, Jones et al. 2013). Progression of theory
63 within the marine environment has been slower due to logistical constraints of collecting
64 comparable data across scales (Kenny et al. 2003, Hinchey et al. 2008, D'Urban Jackson et
65 al. 2020), but has nonetheless emerged to form the discipline of 'seascape ecology' (Pittman
66 et al. 2011).

67 On tropical coral reefs, spatial scales of observation were greatly expanded by the
68 onset of remote sensing technology, permitting their global-scale mapping to a coarse
69 taxonomic resolution (Mumby et al. 1997, Hochberg and Atkinson 2003, Purkis 2018). More
70 recently, *in situ* digital imaging techniques, such as structure-from-motion photogrammetry,
71 have enabled us to study the spatial ecology of coral reef benthic communities at higher
72 taxonomic resolutions (Edwards et al. 2017, Pedersen et al. 2019). Despite these important
73 advances, such data re-introduce the issue of limited sampling extents and previous research
74 has instead tended to focus on comparing spatial patterns across discrete hierarchical scales
75 (Murdoch and Aronson 1999, Williams et al. 2015b). By combining high-resolution digital
76 imagery with towed-diver surveys, recent research has started to reveal the spatial structure of

77 coral reef benthic communities around entire tropical islands (Gove et al. 2015, Aston et al.
78 2019). These data present the opportunity to apply landscape ecological theory and spatial
79 pattern metrics to the marine realm to explore ecological patterns and processes across scales
80 (Wedding et al. 2011).

81 Spatial autocorrelation is a long-standing statistical technique within ecology
82 (Legendre 1993, Cocu et al. 2005) that describes the similarity of a given variable at nearby
83 locations as being greater or less than expected by chance (Fortin et al. 2016). It can be
84 quantified over multiple scales to show how species, habitats and environmental variables are
85 spatially structured. Environmental conditions can be spatially autocorrelated due to several
86 factors, such as climate and geomorphologic processes, which in turn can drive the spatial
87 autocorrelation patterns of ecological communities (Legendre 1993, Gobbi and Brambilla
88 2016).

89 The scale at which spatial autocorrelation is no longer present or changes from being
90 clustered to over-dispersed can indicate a new process acting on biological variables (Zhang
91 and Zhang 2011). Spatial autocorrelation has been used to quantify forest fragmentation
92 (Zhang et al. 2009), optimise sampling protocols for marine macrobenthic invertebrate
93 communities (Hamylton and Barnes 2018) and to relate spatial patterns of insect abundance
94 to environmental gradients (Cocu et al. 2005). On coral reefs, indices of spatial
95 autocorrelation have been used to quantify the spatial patterning of coral bleaching across
96 scales of cm to 100s of m (Levy et al. 2018) and benthic communities up to kilometre-scales
97 around the circumference of a single tropical island (Aston et al. 2019). Despite these recent
98 efforts, our understanding of the patterns of spatial autocorrelation of coral reef communities
99 across scales and geographies remains limited.

100 Here we quantify the spatial scaling properties of tropical benthic communities over
101 ~140 linear km of reef around the circumference of five uninhabited coral reef islands. By

102 processing thousands of *in situ* benthic images and using *in situ* and modelled environmental
103 data, we employ a spatial metric to quantify the patterning of competing functional groups,
104 hard coral morphologies and their suspected physical drivers across scales. Wave energy and
105 subsurface variations in seawater temperature, indicative of intra-island gradients in
106 upwelling (Gove et al., 2006, Aston et al. 2019), can limit or promote the abundance of
107 different benthic groups around tropical islands, including different morphologies (growth
108 forms) of reef-building corals (Williams et al. 2013, Gove et al. 2015). We therefore expect
109 these physical drivers to play a role in the spatial ecology and spatial scaling of tropical
110 benthic communities. Our study objectives were primarily to test whether the intra-island
111 distributions of benthic communities differed from random and if so, up to what scales. We
112 then asked how consistent these spatial scaling properties were across geographies and to
113 what degree they correlated with the spatial scaling of concurrent gradients in physical
114 drivers. Our study therefore establishes important baselines for the spatial ecology of coral
115 reef benthic communities in a world where escalating human interactions with coral reefs
116 (Norström et al. 2016, Hughes et al. 2017, Williams et al. 2019) are fundamentally altering
117 their biological-environmental relationships (Williams et al. 2015a).

118

119 **Methods**

120 **Study sites**

121 Our study system consisted of five U.S.-affiliated coral reef islands and atolls
122 (hereafter referred to as ‘islands’) spanning 6° latitude and 17° longitude in the central Pacific
123 Ocean (Fig. 1): Jarvis Island, Palmyra Atoll, Kingman Reef (Line Islands Archipelago),
124 Howland Island, and Baker Island (U.S. Phoenix Islands). In 1974, Jarvis, Baker and
125 Howland became U.S. National Wildlife Refuges. Kingman and Palmyra were afforded the
126 same protection in 2001. All five islands were declared part of the Pacific Remote Islands

127 Marine National Monument in 2009, further affirming their protected status. Throughout
128 their history, these five islands have lacked permanent human populations and represent some
129 of the most remote coral reef ecosystems on the planet. As such, they offer the opportunity to
130 study the ecology and natural variation of coral reefs in the absence of confounding direct
131 local human impacts (Williams et al. 2015, Heenan et al. 2020), within a relatively similar
132 oceanographic and climatic setting (Gove et al. 2013).

133

134 **Benthic community digital surveys and spatial processing**

135 Digital benthic images were collected around the circumference of each island using
136 towed-diver surveys (Kenyon et al. 2006) in March to April 2008 as part of the National
137 Oceanic and Atmospheric Administration's (NOAA) Pacific Island Fisheries Science
138 Center's (PIFSC) Pacific Reef Assessment and Monitoring Program (RAMP). This survey
139 year was chosen for the present study from the biennial/triennial surveys at each island
140 spanning 2001 to the present due to: 1) representing 10 years of recovery potential following
141 the suspected mass coral bleaching in 1998, and 2) being prior to a bleaching event that
142 affected the region in late 2009 to early 2010 (Williams et al. 2010, Vargas-Ángel et al.
143 2011). As such, this survey year provided the least disturbed benthic community spatial
144 patterns within the time series. Divers manoeuvred a sub-surface instrumented board towed
145 by a surface boat at $\sim 3 \text{ km h}^{-1}$ to target the 15 m depth contour around each island. The tow-
146 board was equipped with a downward facing digital SLR camera (Canon EOS 10-D/50-D)
147 and strobes, taking images every 15 s (equating to every $\sim 15 \text{ m}$) from a height of $\sim 1 \text{ m}$ above
148 the benthos. The average area of the benthos that each survey image captured using this
149 technique was 10.9 m^2 (SE=0.1 m^2 , n=700) (Kenyon et al. 2006).

150 Every alternate image was selected for subsequent analyses and images were filtered
151 to only include those within a depth range of 8 – 20 m on the forereef habitat (reef slope

152 facing the open ocean) of each island to ensure comparability with prior studies in the
153 region (Gove et al. 2015, Williams et al. 2015a, Aston et al. 2019). We used the analysis
154 software CoralNet (Beijbom et al. 2015) to overlay 10 points in a stratified-random design
155 over each photo and identify the benthos below each as either: hard coral (to morphology),
156 macroalgae, soft coral, crustose coralline algae, turf algae, other invertebrates (echinoderm,
157 bivalve, zoanthid, anemone, corallimorph), and bare sand (for detailed descriptions of
158 functional groups and coral morphologies see Supplementary material Appendix 1, Table A1
159 and A2).

160 A Global Positioning System (GPS) aboard the boat timestamped to the camera and a
161 SeaBird™ Electronics (SBE) 39 subsurface pressure, temperature-depth recorder on the tow-
162 board, combined with a layback algorithm (Kenyon et al. 2006), allowed each photograph to
163 be georeferenced to the nearest ~3 – 5 m and depth referenced. For the few instances where
164 depth data were missing, we used an interpolation based on inverse distance weighting using
165 the Spatial Analyst tool in ArcGIS (v 10.7.1) and matched the missing depths to interpolated
166 depth data from the same island area from surveys in 2006 and 2010. Each island's
167 circumference was divided into a series of discrete, sequentially numbered grid cells (100 m
168 wide) using a custom Python script (*sensu* Aston et al. 2019, <<https://doi.org/10.5281/zenodo.1199350>>); the number of grid cells around each island ranged from
169 77 to 340. Benthic image data were spatially joined to each grid cell and, to be included in
170 further spatial analyses, grid cells had to contain ≥ 4 benthic images (*sensu* Aston et al.
171 2019). To help satisfy this prerequisite and maximise spatial coverage around each island, for
172 those grid cells with < 4 images we revisited our initial filtering step (where we excluded
173 every alternate image) and re-selected some images for processing. In total, we processed
174 6022 images across the five islands (Howland, 787; Baker, 838; Jarvis, 1107; Kingman,
175 1560; Palmyra, 1730) to calculate a mean cover value for each benthic variable per grid cell,
176

177 with 77% to 96% of grid cells containing data around the five islands (see Supplementary
178 Material Appendix 1, Table A3).

179

180 **Quantifying physical drivers**

181 We calculated surface wave power using a 3-hr output at 50 km resolution from
182 NOAA's Wave Watch III global model (WWIII; <<http://polar.ncep.noaa.gov/waves>>). Wave
183 power (W m^{-1}) was calculated from significant wave height (H_s) and peak period (T_p),
184 defined as:

$$185 \quad WP = \frac{\rho g^2 T_p H_s^2}{64\pi}$$

186 where ρ is the density of seawater (1024 kg m^{-3}) and g is the acceleration of gravity (9.8 m s^{-2}). From this output, calculations using an incident wave swath method (*sensu* Aston et al.
187 2019) estimated the wave power at regularly spaced locations (between on island) around
188 each island, ranging from ~100 – 500 m depending on island size We calculated an integrated
189 10-yr average (1998 – 2008) in wave energy flux (kW hr m^{-1}) for each location and used a
190 250 m radial buffer around each location to spatially join to the 100 m grid cells, averaging
191 values within cells that contained multiple overlapping buffers.

192
193 *In situ* seawater temperature was recorded during each towed-diver survey in 2008
194 using the SBE39 logger attached to the towboard (10 s sample rate, 0.002 °C accuracy).
195 Despite being a temporal snapshot, these *in situ* temperature data capture long-term intra-
196 island gradients in sub-surface temperature that are indicative of localised upwelling (Gove et
197 al. 2006). Like the benthic and wave data, we spatially joined the subsurface temperature data
198 to each discrete island grid cell and calculated a mean value per cell.

199

200 **Spatial statistics and sensitivity analyses**

201 To quantify changes in the spatial autocorrelation of benthic communities and their
 202 physical drivers across scales, we used the Moran’s I statistic (Moran 1950) twithin a custom-
 203 coded function (Aston et al. 2019) in the R programming language (R Core Team 2019), and
 204 which we build upon here to allow the comparison of these patterns across islands. When
 205 calculating the Moran’s I statistic for hard coral morphologies, we selected the two to three
 206 most abundant morphologies at each island. We defined the observed Moran’s I value (OMI)
 207 as:

$$208 \quad I = \frac{n \sum_{i=1}^n \sum_{j=1}^n w_{i,j} (x_i - \bar{x})(x_j - \bar{x})}{S_0 \sum_{i=1}^n (x_i - \bar{x})^2}$$

209 where n is the number of observations, $w_{i,j}$ is the matrix of weights according to the inverse
 210 Euclidean distance between observations, x_i is the observed value at location i , x_j is the
 211 observed value at location j , \bar{x} is the mean value and S_0 is the sum of spatial weights. The
 212 spatial weights are defined as the inverse of the minimum distance, $d_{i,j}$, around the
 213 circumference of each island between locations i and j , as follows:

$$214 \quad d_{i,j} = \min((j - i), (n + i - j))$$

$$215 \quad w_{i,j} = \frac{1}{d_{i,j}} \text{ for } i \neq j, 0 \text{ otherwise}$$

216 A significant ($p < 0.05$) departure from an OMI value of zero (i.e. away from a random
 217 distribution) indicated that the spatial pattern of the variable in question at that scale was
 218 highly organised in space. Positive OMI values indicated positive autocorrelation (i.e. spatial
 219 clustering), while negative OMI values indicated negative autocorrelation (i.e. over-
 220 dispersion). We calculated the Moran’s I statistic at the finest spatial resolution of the data
 221 (100 m grid cells), and then again in a moving window averaging process at increasing 100-m
 222 increments to a maximum scale of 4 km (limited by replication beyond that scale due to
 223 island size). Grid cells containing ‘no data’ (i.e. $<$ four benthic images) were excluded from
 224 the moving window averaging process. As spatial patterns in nature can be anisotropic, at

225 each scale we re-computed the Moran's I statistic and p-value for all possible 100 m grid cell
226 starting locations of the moving window averaging process and iterating in both directions
227 around the circumference of each island. We report the mean, maximum and minimum OMI
228 value for each scale from this process and the scale at which the upper bound of p exceeded
229 0.05 (i.e. did not differ significantly from a random spatial distribution).

230 As the number of grid cells with 'no data' varied across islands (Fig.1), we performed
231 a series of sensitivity analyses to quantify the possible impact this might have on our
232 comparison of spatial autocorrelation patterns. At Kingman, 21% of grid cells had 'no data'
233 (81 out of 380). For the other islands, we assigned 'no data' values to grid cells at random
234 until we reached the same ratio of missing data as Kingman, then repeated our moving
235 window averaging process and recalculated the Moran's I statistic. We repeated this at each
236 island 100 times, each time randomising the 'no data' grid cell locations. From the iterations,
237 we calculated a mean re-sampled OMI and p-value and identified the smallest and largest
238 scale at which $p \geq 0.05$ (see Supplementary material Appendix 1, Fig. A1).

239

240 **Results**

241 **The spatial scaling of coral reef benthic communities across geographies**

242 The spatial distribution of benthic functional groups appeared non-random around the
243 circumference of each island, with some groups dominating large expanses of coastlines for
244 several km (Fig. 1). On occasion, these regions of spatial dominance showed consistencies
245 between islands. For example, macroalgae was spatially clumped along the southeast coast of
246 Kingman and the south coast of neighbouring Palmyra, reaching 11 – 46% cover over a 1.8
247 km stretch of coastline at Kingman and 25 – 68% along a 1.5 km stretch at Palmyra (Fig. 1).
248 Different coral morphologies also exhibited non-random distributions, and again displayed
249 discrete zones of spatial dominance along coastlines (Fig. 1). For example, plating coral

250 peaked at 70% cover and dominated 1.2 km of Kingman’s south coast, while branching coral
251 cover dominated the northeast coast of neighbouring Howland and Baker for 1.1 km and 1.2
252 km, respectively (Fig.1).

253 All benthic functional groups displayed strong evidence of spatial clustering (positive
254 autocorrelation) around the circumference of each island, but the scale and strength of this
255 autocorrelation differed between islands (Fig. 2). Around Howland, crustose coralline algae
256 (CCA) and turf algae showed positive spatial autocorrelation at scales up to 0.3 km and CCA
257 had similar spatial clustering at neighbouring Baker. Around Kingman, Jarvis and Baker, turf
258 algae were spatially clustered across the seascape at scales of ~1 km. Macroalgae and hard
259 corals displayed comparable scaling patterns at neighbouring Howland and Baker; both
260 groups were spatially clustered at scales up to ~500 m at Howland and ~1 km at Baker. These
261 inter-island spatial autocorrelation patterns were robust to variations in the number and
262 spatial distribution of grid cells containing no data; the scales at which benthic functional
263 groups significantly differed from random only changed by up to 100 m (see Supplementary
264 material Appendix 1, Fig. A1). Macroalgae were the most spatially clustered of any
265 functional group at the finest resolution of our data (100 m), having a consistently high
266 Observed Moran’s I Index of ~0.4 around Baker, Kingman and Palmyra (Fig. 2). However,
267 the spatial distribution of macroalgae at Jarvis did not differ from random at any scale, likely
268 due to its low island-mean cover of 1.8% (almost 3 times lower than at Kingman, the island
269 with the next lowest abundance).

270 Different coral morphologies also showed strong evidence of spatial clustering around
271 the circumference of each island, with some consistencies in scaling between morphologies
272 of the same type at different islands (Fig. 3). At neighbouring Howland and Baker, branching
273 corals were spatially clustered up to scales of 700 – 800 m and followed a similar gradient in
274 spatial autocorrelation across scales (Fig. 3). The scaling of encrusting corals was also similar

275 between Kingman, Howland and Palmyra, being spatially clustered up to scales of 1.1 – 1.3
276 km (Fig. 3). Branching corals at Howland and Baker and plating corals at Jarvis had their
277 highest degree of spatial clustering at the finest spatial resolution (100 m) (Fig. 3). In
278 contrast, plating corals at other islands, as well as submassive, corymbose and encrusting
279 coral morphologies, peaked in autocorrelation at a 200 m scale, suggesting a less clustered
280 distribution at smaller spatial scales (Fig. 3).

281

282 **Correlation between the spatial scaling properties of benthic communities and their** 283 **physical drivers**

284 There were cases where the upper scale of significant spatial clustering remained
285 similar between benthic community members and the physical drivers. At the functional
286 group resolution, this overall correlation was stronger for wave energy ($\rho= 0.73$) than for
287 subsurface temperature ($\rho= 0.46$) as well as individually for any single benthic functional
288 group ($\rho= 0.71 – 0.93$ for wave energy, $0.37 – 0.82$ for subsurface temperature) (Fig. 4) (see
289 Supplementary material Appendix 1 Fig. A2 for spatial autocorrelation patterns in wave
290 energy and subsurface temperature across scales). There was also inter-island variability in
291 this alignment. For example, around Baker, wave energy was spatially clustered up to scales
292 of ~1 km and turf algae, macroalgae and hard coral were also clustered up to ~1 km. Around
293 Kingman, subsurface temperature and turf algae were both spatially clustered up to ~1 km,
294 while wave energy and hard coral cover were both clustered up to scales of ~2.4 km. In
295 contrast, there was consistently poor alignment at Palmyra, with none of the upper scales of
296 significant autocorrelation in the benthic functional groups closely resembling those of the
297 physical drivers (Fig. 4).

298 The correlation between the upper scale at which there remained significant spatial
299 autocorrelation in the benthos and physical drivers was not as strong for hard coral

300 morphologies ($\rho= 0.50$ and 0.46 for wave energy and subsurface temperature, respectively).
301 There was substantial variation across the different coral morphologies, with some showing
302 closer alignment to the physical drivers than others. For example, the spatial scaling of
303 plating corals closely matched those of wave energy regardless of island, and some coral
304 morphologies appeared to be more closely aligned at specific islands than others (Fig. 5).
305 Encrusting corals around Howland were spatially clustered up to 1.1 km, exactly matching
306 the spatial scaling of subsurface temperature and wave energy. At Jarvis, plating corals were
307 clustered up to 1.4 km, similar to the spatial clustering exhibited by both subsurface
308 temperature and wave energy (to within 200 m). Finally, at Kingman, encrusting and
309 submassive corals and subsurface temperature were spatially clustered up to scales of ~ 1 km,
310 while plating corals and wave energy were both clustered up to ~ 2 km scales (Fig. 5).

311

312 **Discussion**

313

314 **The autocorrelated nature of coral reef seascapes**

315 Our results show that coral reef benthic communities are naturally spatially clustered
316 across tropical island seascapes, with individual groups in some cases dominating entire km-
317 sections of coastline (Fig. 1). Structural complexity of benthic assemblages can be influenced
318 by the dominant functional group or coral morphology, which will have an effect on the
319 spatial structure of reef-associated organisms, including fish communities (Alvarez-Filip et
320 al. 2011, Richardson et al. 2017). Furthermore, these sections of dominance are evidence that
321 ‘ecotones’ – discrete transition points between two communities or habitat types – exist
322 around these tropical oceanic islands, which will likely have structuring effects on reef-
323 associated organisms, akin to those of forest edges (Pfeifer et al. 2017) and coral reef-
324 seagrass transition zones (Dorenbosch et al. 2005). Acknowledging the autocorrelated nature

325 of coral reef benthic communities, may have important management implications. For
326 example, larger patches dominated by hard coral of a structurally complex morphology with a
327 seagrass-hard coral ecotone, may be more beneficial to maintain ecosystem structure and
328 function. Such patterns of naturally occurring spatial autocorrelation should be considered in
329 marine spatial planning and coral restoration efforts that may attempt to mimic the inherent
330 spatial properties of coral reefs.

331 The spatial scaling patterns of benthic groups differed across geographies but had the
332 common attribute of displaying positive spatial autocorrelation up to several kilometres of
333 scale across all five study islands. Previously, Bradbury and Young (1983) found corals to be
334 spatially clumped at 60-m scales across shallow reef flats and reef crests of the Great Barrier
335 Reef in Australia. Edwards et al. (2017) also found most coral taxa were spatially clustered
336 within 100 m² plots at 10 m depth on the outer reef slope of Palmyra Atoll, central Pacific
337 (one of our study islands). We found the highest levels of positive autocorrelation in all
338 benthic community members at our smallest spatial scales (100 – 200 m) around all five of
339 our study islands. We therefore hypothesise that positive autocorrelation, particularly at
340 smaller scales, is a common spatial attribute of corals and other benthic organisms across
341 depths, reef habitats, and geographies.

342

343 **Drivers of coral reef benthic community seascapes**

344 The non-random spatial dominance of benthic functional groups and hard coral
345 morphologies around kilometre-sections of our five study islands likely exist, in part, because
346 of concurrent gradients in the physical environment. Physical environmental drivers are key
347 determinants of benthic community structure around oceanic islands, promoting or limiting
348 the abundance of competitors particularly in the absence of local human impacts (Gove et al.
349 2015, Williams et al. 2015a). Howland, Baker and Jarvis have pronounced cross-island

350 gradients in subsurface temperature, reflective of localised upwelling along their western
351 coasts that results in the up-slope movement of deep, cold, nutrient-rich waters onto shallow
352 reef communities (Gove et al. 2006, Tsuda et al. 2008, Aston et al. 2019). Algae can benefit
353 from increased growth under high nutrient conditions on coral reefs (Littler et al. 1983, Miller
354 et al. 1999), which may explain spatial clustering of turf algae and macroalgae along
355 continuous km-scale sections of Baker and Howland's western coasts, respectively. As well
356 as benefiting algae, upwelling can enhance growth rates in reef-building corals (Diaz-Pulido
357 and Garzón-Ferreira 2002, Edmunds and Leichter 2016) by providing heterotrophic energetic
358 subsidies (Williams et al. 2018). In some cases, this can give corals a competitive advantage
359 over algae and strong upwelling is thought to explain the kilometre-sections of hard coral
360 dominance along the western coast of Jarvis (Aston et al. 2019).

361 Like competing benthic functional groups, individual hard coral morphologies
362 displayed strong spatial clustering along kilometre-sections of the island coastlines that are
363 also likely driven, in part, by gradients in physical drivers. Our results indicate that the high
364 spatial clustering of hard coral along the western coast of Jarvis, a more wave-sheltered part
365 of the island, is almost exclusively dominated by plating coral. Plating and branching corals
366 are susceptible to breakage and dislodgement by high wave energy (Madin et al. 2014),
367 whereas encrusting, digitate and massive coral morphologies are more wave-resistant and
368 dominate in more wave-exposed areas (Gove et al. 2015). Branching corals also dominated
369 sections of Howland and Baker's north-eastern to south-eastern coasts, which are sheltered
370 from winter storm swells from the north-west (Mundy et al. 2010). In contrast, Palmyra's
371 northern coast is exposed to north-west winter swells (Williams et al. 2013) and here we saw
372 spatial clustering of more wave-tolerant encrusting and corymbose corals.

373 Benthic functional groups not only dominated km-sections of island coastlines, but
374 also showed non-random patterns of spatial clustering across scales (Fig. 2, 3). In some cases,

375 the upper scale at which benthic functional groups were spatially clustered around islands
376 closely correlated with the upper scale at which the physical drivers were spatially clustered
377 (Fig. 4). This correlation was more evident with wave energy than subsurface temperature
378 regardless of functional group, and across functional groups, the strongest correlations with
379 the physical drivers were evident in turf algae and CCA. High wave energy often favours
380 low-lying, wave-tolerant algae, such as turf and CCA and limits the dominance of larger
381 upright macroalgae that, like some corals, are vulnerable to dislodgement (Page-Albins et al.
382 2012, Williams et al. 2013, Gove et al. 2015). Our findings show, for the first time, that
383 physical drivers on coral reefs not only limit or promote the abundance of individual benthic
384 groups, but also play a key role in governing their spatial scaling properties across tropical
385 seascapes.

386 The spatial scaling of coral reef benthic communities was more similar between
387 islands closer in proximity and size. For example, at neighbouring Kingman and Palmyra (63
388 km apart), macroalgae were spatially structured up to ~3 km scales at both islands. At
389 neighbouring Howland and Baker (69 km apart), CCA was spatially structured up to scales of
390 0.3 km at both islands. We hypothesise that these common benthic scaling patterns between
391 closely situated islands reflect broader-scale autocorrelation in environmental conditions that
392 exist across archipelagos, with islands in closer proximity exposed to similar surrounding
393 environmental conditions (Gove et al. 2013). Kingman and Palmyra also have much larger
394 total reef areas and longer coastlines, producing more expansive areas of reef slope of the
395 same aspect, than at the other three islands (Gove et al. 2016). This may allow environmental
396 homogeneity over greater linear extents, particularly with regards to incoming wave energy
397 and could give rise to the large homogeneous zones of spatial dominance by single benthic
398 functional groups and coral morphologies that we observe at Kingman and Palmyra. Smaller

399 coastlines and total reef areas at Howland, Baker and Jarvis could explain why benthic
400 functional groups here, only remained spatially clustered at smaller spatial scales.

401 Our results support the expectation that environmental drivers can cause ecological
402 responses at larger spatial scales, while biotic factors drive smaller-scale patterns and
403 processes (Legendre 1993). We found the upper bounds in scale at which the benthic and
404 physical variables showed spatial clustering were highly correlated, suggesting that physical
405 drivers set the upper spatial bound in which benthic communities are spatially organised
406 around tropical oceanic islands. At smaller spatial scales (100 – 200 m), we saw the highest
407 degree of benthic community spatial clustering, which may be better explained by biotic
408 factors. For example, the dominant macroalgae around our study islands are calcifying
409 *Halimeda* (Vroom et al. 2010, Williams et al. 2013) that reproduce asexually over short
410 distances by fragmentation. This type of reproduction could explain the high degrees of
411 macroalgal spatial clustering at scales of 100 – 200 m around Kingman, Palmyra, Howland
412 and Baker. Similarly, the high spatial clustering of branching corals at smaller scales at
413 Howland and Baker, could be explained by the branching corals all being fast-growing
414 Acroporids that can also reproduce over short distances through fragmentation (Baird and
415 Hughes 2000).

416

417 **Conclusion**

418 For the first time, we quantify the autocorrelated nature of coral reef seascapes across
419 geographies in the absence of direct local human impacts. All major benthic functional
420 groups and hard coral morphologies showed evidence of positive autocorrelation (spatial
421 clustering) up to scales of 0.3 to 3.5 km around the circumference of five oceanic tropical
422 islands. The scales across which benthic community members exhibited spatial structure and
423 the strength of these autocorrelation patterns differed between islands but was more similar

424 between islands closer in proximity and of a similar size. In some cases, benthic community
425 spatial scaling was similar to the scaling of concurrent gradients in physical drivers, in
426 particular wave energy. This suggests that physical drivers not only play a role in governing
427 patterns of community abundance on tropical coral reefs, but also contribute to determining
428 their spatial scaling properties across the seascape. How these patterns of biological
429 autocorrelation change in response to changes in physical gradients, such as those that occur
430 during environmental disturbance events, remains unknown and is an exciting avenue for
431 future research.

432

433 **Acknowledgements**

434 We thank NOAA's Pacific Islands Fisheries Science Center (PIFSC) Ecosystem Sciences
435 Division and the officers and crews of the NOAA ships Hi'ialakai and Oscar Elton Sette for
436 coordinating and conducting all towed-diver surveys. HVF was supported by a Envision
437 Doctoral Training Programme scholarship funded by the National Environment Research
438 Council (NERC) of the U.K. and co-funding from The Nature Conservancy. We thank
439 members of the Reef Systems Lab at Bangor University's School of Ocean Sciences for their
440 collective advice towards project development, the NOAA internal review process and two
441 anonymous reviewers for their helpful comments on the manuscript draft, and Amanda
442 Dillon at Aline Design for help with figure formatting.

443

444 Author contributions – HVF and GJW conceived the study; HVF analysed the data with
445 GJW, JMG and AJD; HVF wrote the manuscript with GJW. All authors contributed to the
446 editing of the manuscript.

447

448

449 **References**

- 450 Addicott, J. F. et al. 1987. Ecological Neighborhoods: Scaling Environmental Patterns. -
451 *Oikos* 49: 340.
- 452 Alvarez-Filip, L. et al. 2011. Complex reef architecture supports more small-bodied fishes
453 and longer food chains on Caribbean reefs. - *Ecosphere* 2: 1–17.
- 454 Aston, E. A. et al. 2019. Scale-dependent spatial patterns in benthic communities around a
455 tropical island seascape. - *Ecography*. 42: 578–590.
- 456 Baird, A. H. and Hughes, T. P. 2000. Competitive dominance by tabular corals: an
457 experimental analysis of recruitment and survival of understory assemblages. - *J. Exp.*
458 *Mar. Bio. Ecol.* 251: 117–132.
- 459 Beijbom, O. et al. 2015. Towards Automated Annotation of Benthic Survey Images:
460 Variability of Human Experts and Operational Modes of Automation. - *PLoS One* 10:
461 e0130312.
- 462 Boström, C. et al. 2011. Seascape ecology of coastal biogenic habitats: advances, gaps, and
463 challenges. - *Mar. Ecol. Prog. Ser.* 427: 191–217.
- 464 Bradbury, R. and Young, P. 1983. Coral interactions and community structure: an analysis of
465 spatial pattern. - *Mar. Ecol. Prog. Ser.* 11: 265–271.
- 466 Cocu, N. et al. 2005. Spatial autocorrelation as a tool for identifying the geographical patterns
467 of aphid annual abundance. - *Agric. For. Entomol.* 7: 31–43.
- 468 D'Urban Jackson, T. et al. 2020. Three-dimensional digital mapping of ecosystems: a new
469 era in spatial ecology. - *Proc. R. Soc. B Biol. Sci.* 287: 20192383.
- 470 De Knegt, H. J. et al. 2011. The spatial scaling of habitat selection by African elephants. - *J.*
471 *Anim. Ecol.* 80: 270–281.
- 472 Diaz-Pulido, G. and Garzón-Ferreira, J. 2002. Seasonality in algal assemblages on upwelling-
473 influenced coral reefs in the Colombian Caribbean. - *Bot. Mar.* 45: 284–292.

474 Dorenbosch, M. et al. 2005. Distribution of coral reef fishes along a coral reef-seagrass
475 gradient: Edge effects and habitat segregation. - *Mar. Ecol. Prog. Ser.* 299: 277–288.

476 Dungan, J. L. et al. 2002. A balanced view of scale in spatial statistical analysis. - *Ecography*.
477 25: 626–640.

478 Edmunds, P. J. and Leichter, J. J. 2016. Spatial scale-dependent vertical zonation of coral reef
479 community structure in French Polynesia. - *Ecosphere* 7: e01342.

480 Edwards, C. B. et al. 2017. Large-area imaging reveals biologically driven non-random
481 spatial patterns of corals at a remote reef. - *Coral Reefs*. 36: 1291-1305

482 Estes, L. et al. 2018. The spatial and temporal domains of modern ecology. - *Nat. Ecol. Evol.*
483 2: 819–826.

484 Fortin, M.-J. et al. 2016. *Spatial Analysis in Ecology*. - In: *Wiley StatsRef: Statistics*
485 *Reference Online*. John Wiley & Sons, Ltd, pp. 1–13.

486 Gobbi, M. and Brambilla, M. 2016. Patterns of spatial autocorrelation in the distribution and
487 diversity of carabid beetles and spiders along Alpine glacier forelands. - *Ital. J. Zool.* 83:
488 600–605.

489 Gove, J. M. et al. 2006. Temporal variability of current-driven upwelling at Jarvis Island. - *J.*
490 *Geophys. Res.* 111: C12011.

491 Gove, J. M. et al. 2013. Quantifying Climatological Ranges and Anomalies for Pacific Coral
492 Reef Ecosystems. - *PLoS One* 8: e61974.

493 Gove, J. M. et al. 2015. Coral reef benthic regimes exhibit non-linear threshold responses to
494 natural physical drivers. 522: 33–48.

495 Gove, J. M. et al. 2016. Near-island biological hotspots in barren ocean basins. - *Nat.*
496 *Commun.* 7: 1–8.

497 Hamylton, S. M. and Barnes, R. S. K. 2018. The effect of sampling effort on spatial
498 autocorrelation in macrobenthic intertidal invertebrates. - *Hydrobiologia* 811: 239–250.

499 Hatcher, B. G. et al. 1987. Scaling analysis of coral reef systems: an approach to problems of
500 scale. - *Coral Reefs* 5: 171–181.

501 Heenan, A. et al. 2020. Natural variation in coral reef trophic structure across environmental
502 gradients. - *Front. Ecol. Environ.* 18: 69–75.

503 Hinchey, E. K. et al. 2008. Preface: Marine and coastal applications in landscape ecology. -
504 *Landsc. Ecol.* 23: 1–5.

505 Hochberg, E. J. and Atkinson, M. J. 2003. Capabilities of remote sensors to classify coral,
506 algae, and sand as pure and mixed spectra. - *Remote Sens. Environ.* 85: 174–189.

507 Hughes, T. P. et al. 2017. Coral reefs in the Anthropocene. - *Nature* 546: 82–90.

508 Jones, K. B. et al. 2013. Informing landscape planning and design for sustaining ecosystem
509 services from existing spatial patterns and knowledge. - *Landsc. Ecol.* 28: 1175–1192.

510 Kenny, A. et al. 2003. An overview of seabed-mapping technologies in the context of marine
511 habitat classification. - *ICES J. Mar. Sci.* 60: 411–418.

512 Kenyon, J. C. et al. 2006. Towed-Diver Surveys, a Method for Mesoscale Spatial Assessment
513 of Benthic Reef Habitat: A Case Study at Midway Atoll in the Hawaiian Archipelago. -
514 *Coast. Manag.* 34: 339–349.

515 Lee, M. F. et al. 2008. Remote sensing assessment of forest damage in relation to the 1996
516 strong typhoon Herb at Lienhuachi Experimental Forest, Taiwan. - *For. Ecol. Manage.*
517 255: 3297–3306.

518 Legendre, P. 1993. Spatial Autocorrelation: Trouble or New Paradigm? - *Ecology* 74: 1659–
519 1673.

520 Levin, S. A. 1992. The Problem of Pattern and Scale in Ecology: The Robert H. MacArthur
521 Award Lecture. - *Ecology* 73: 1943–1967.

522 Levy, J. et al. 2018. Assessing the spatial distribution of coral bleaching using small
523 unmanned aerial systems. - *Coral Reefs* 37: 373–387.

524 Littler, M. M. et al. 1983. Evolutionary strategies in a tropical barrier reef system:
525 Functional-form groups of marine macroalgae. - *J. Phycol.* 19: 229–237.

526 Madin, J. S. et al. 2014. Mechanical vulnerability explains size-dependent mortality of reef
527 corals. - *Ecol. Lett.* 17: 1008–1015.

528 Miller, M. W. et al. 1999. Effects of nutrients versus herbivores on reef algae: A new method
529 for manipulating nutrients on coral reefs. - *Limnol. Oceanogr.* 44: 1847–1861.

530 Moran, P. A. P. 1950. Notes on Continuous Stochastic Phenomena. - *Biometrika* 37: 17.

531 Mumby, P. J. et al. 1997. Coral reef habitat-mapping: How much detail can remote sensing
532 provide? - *Mar. Biol.* 130: 193–202.

533 Mundy, B. C. et al. 2010. Inshore Fishes of Howland Island, Baker Island, Jarvis Island,
534 Palmyra Atoll, and Kingman Reef. - *Atoll Res. Bull.* 585

535 Murdoch, T. J. T. and Aronson, R. B. 1999. Scale-dependent spatial variability of coral
536 assemblages along the Florida Reef Tract. - *Coral Reefs* 18: 341–351.

537 Nash, K. L. et al. 2014. Discontinuities, cross-scale patterns, and the organization of
538 ecosystems. - *Ecology* 95: 654–667.

539 Norström, A. V et al. 2016. Guiding coral reef futures in the Anthropocene. - *Front. Ecol.*
540 *Environ.* 14: 490–498.

541 Page-Albins, K. N. et al. 2012. Patterns in Benthic Coral Reef Communities at Pearl and
542 Hermes Atoll along a Wave-Exposure Gradient. - *Pacific Sci.* 66: 481–496.

543 Pedersen, N. E. et al. 2019. The influence of habitat and adults on the spatial distribution of
544 juvenile corals. - *Ecography.* 42: 1703–1713.

545 Pfeifer, M. et al. 2017. Creation of forest edges has a global impact on forest vertebrates. -
546 *Nature* 551: 187–191.

547 Pittman, S. J. et al. 2011. Practicing coastal seascape ecology. - *Mar. Ecol. Prog. Ser.* 427:
548 187–190.

549 Purkis, S. J. 2018. Remote Sensing Tropical Coral Reefs: The View from Above. - *Ann. Rev.*
550 *Mar. Sci.* 10: 149–168.

551 R Core Team 2019. R: A language and environment for statistical computing.

552 Rahbek, C. and Graves, G. R. 2000. Detection of macro-ecological patterns in South
553 American hummingbirds is affected by spatial scale. - *Proc. R. Soc. B Biol. Sci.* 267:
554 2259–2265.

555 Richardson, L. E. et al. 2017. Structural complexity mediates functional structure of reef fish
556 assemblages among coral habitats. - *Environ. Biol. Fishes* 100: 193–207.

557 Schneider, D. C. 1994. *Quantitative Ecology: Spatial and Temporal Scaling*. - Elsevier.

558 Schneider, D. C. 2001. The rise of the concept of scale in ecology. - *Bioscience* 51: 545–553.

559 Tsuda, R. T. et al. 2008. Additional Marine Benthic Algae from Howland and Baker Islands,
560 Central Pacific 1. - *Pacific Sci.* 62: 271–290.

561 Vargas-Ángel, B. et al. 2011. Severe, Widespread El Niño–Associated Coral Bleaching in the
562 US Phoenix Islands. - *Bull. Mar. Sci.* 87: 623–638.

563 Vroom, P. S. et al. 2010. Marine biological community baselines in unimpacted tropical
564 ecosystems: Spatial and temporal analysis of reefs at Howland and Baker Islands. -
565 *Biodivers. Conserv.* 19: 797–812.

566 Wagner, H. H. and Fortin, M.-J. 2005. Spatial analysis of landscapes: concepts and statistics.
567 - *Ecology* 86: 1975–1987.

568 Wedding, L. M. et al. 2011. Quantifying seascape structure: Extending terrestrial spatial
569 pattern metrics to the marine realm. - *Mar. Ecol. Prog. Ser.* 427: 219–232.

570 Wiens, J. A. and Milne, B. T. 1989. Scaling of “landscapes” in landscape ecology, or,
571 landscape ecology from a beetle’s perspective. - *Landsc. Ecol.* 3: 87–96.

572 Williams, G. J. et al. 2010. Modeling patterns of coral bleaching at a remote Central Pacific
573 atoll. - *Mar. Pollut. Bull.* 60: 1467–1476.

- 574 Williams, G. J. et al. 2013. Benthic communities at two remote Pacific coral reefs: Effects of
575 reef habitat, depth, and wave energy gradients on spatial patterns. - PeerJ 2013: 1–26.
- 576 Williams, G. J. et al. 2015a. Local human impacts decouple natural biophysical relationships
577 on Pacific coral reefs. - Ecography. 38: 751–761.
- 578 Williams, S. M. et al. 2015b. Hierarchical spatial patterns in Caribbean reef benthic
579 assemblages. - J. Biogeogr. 42: 1327–1335.
- 580 Williams, G. J. et al. 2018. Biophysical drivers of coral trophic depth zonation. - Mar. Biol.
581 165: 60.
- 582 Williams, G. J. et al. 2019. Coral reef ecology in the Anthropocene. - Funct. Ecol. 33: 1014–
583 1022.
- 584 Zhang, N. and Zhang, H. 2011. Scale variance analysis coupled with Moran's *I* scalogram to
585 identify hierarchy and characteristic scale. - Int. J. Geogr. Inf. Sci. 25: 1525–1543.
- 586 Zhang, X. et al. 2009. NDVI spatial pattern and its differentiation on the Mongolian Plateau. -
587 J. Geogr. Sci. 19: 403–415.

588

589 **Figure captions**

590

591 **Figure 1.** Spatial variations in percentage cover of coral reef benthic functional groups and
592 dominant hard coral morphologies on the outer reef slopes (~15 m depth) of five uninhabited
593 central Pacific islands collected via towed-diver digital image surveys in 2008 across ~140
594 linear km of reef (n = 6022 images). The white cells around each island are 100-m grid cells
595 that overlap the towed-diver tracks and are used to spatially reference individual images (their
596 numbers start due north and correspond with those on the island rosette plots). Grey regions on
597 the rosette plots represent missing data regions. The islands are ordered in increasing size top
598 to bottom.

599

600 **Figure 2.** Patterns of spatial autocorrelation (solid coloured line) in the percentage cover of
601 benthic functional groups at increasing 100-m scale increments around five uninhabited
602 central Pacific islands. The Observed Moran's I (OMI) value indicates a clustered
603 distribution (+ve values), random distribution (0 value, horizontal dotted line) to increasingly
604 dispersed (-ve values). The OMI is calculated for all possible starting points around each
605 island and the range in these values for each scale is shown as the shaded region. The vertical
606 dotted line shows the scale at which the OMI value is not significantly different from random
607 for each benthic group ($p \geq 0.05$). CCA, crustose coralline algae.

608

609 **Figure 3.** Patterns of spatial autocorrelation (solid coloured line) in the percentage cover of
610 dominant hard coral morphologies at increasing 100-m scale increments around five
611 uninhabited central Pacific islands. The Observed Moran's I (OMI) value indicates a clustered
612 distribution (+ve values), random distribution (0 value, horizontal dotted line) to increasingly
613 dispersed (-ve values). The OMI is calculated for all possible starting points around each island
614 and the range in these values for each scale is shown as the shaded region. The vertical dotted
615 line shows the scale at which the OMI value is not significantly different from random for each
616 benthic group ($p \geq 0.05$).

617

618 **Figure 4.** Correlation between the upper scale at which there remained significant spatial
619 clustering in the benthic functional groups and physical drivers around five uninhabited
620 central Pacific islands (diagonal dotted line is a 1:1 reference). Overall Spearman Rank
621 correlation coefficient (ρ) equaled 0.73 for wave energy and 0.46 for subsurface temperature.
622 Correlation values for each individual benthic functional group and wave energy equaled:
623 crustose coralline algae (CCA) = 0.81, turf algae = 0.93, hard coral = 0.71, macroalgae =

624 0.79), and for subsurface temperature equaled: CCA = 0.48, turf algae = 0.82, hard coral =
625 0.37, macroalgae = 0.47).

626

627 **Figure 5.** Correlation between the upper scale at which there remained significant spatial
628 clustering in the dominant hard coral morphologies and physical drivers around five
629 uninhabited central Pacific islands (diagonal dotted line is a 1:1 reference). Overall Spearman
630 Rank correlation coefficient (ρ) equaled 0.50 for wave energy and 0.46 for subsurface
631 temperature. Note that unlike in Fig. 4, correlation values for individual morphologies are not
632 calculated due to a lack of adequate replication across islands.

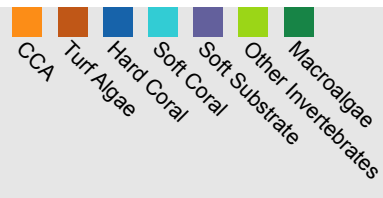
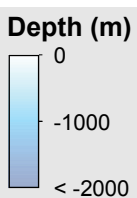
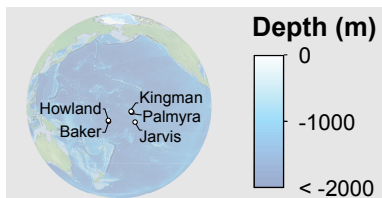
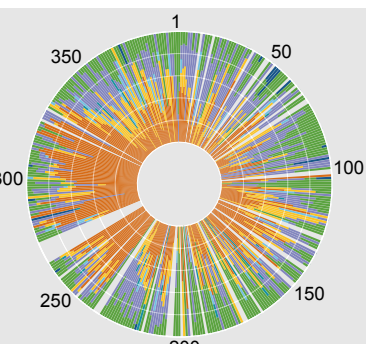
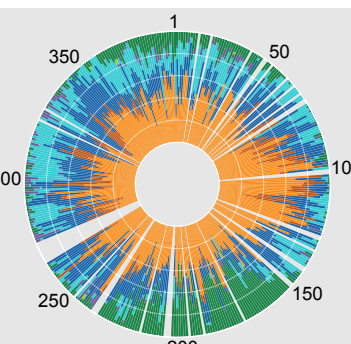
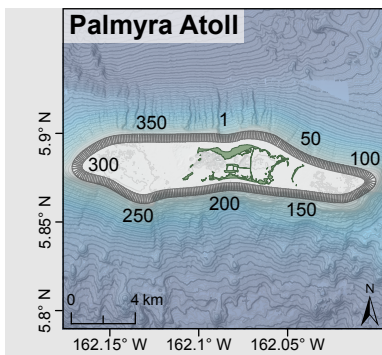
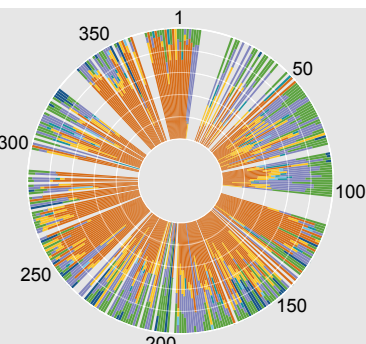
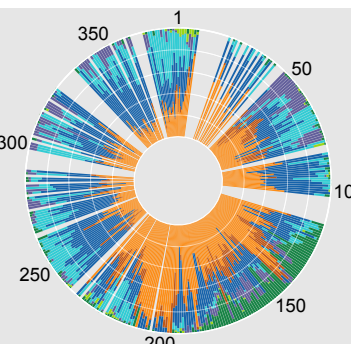
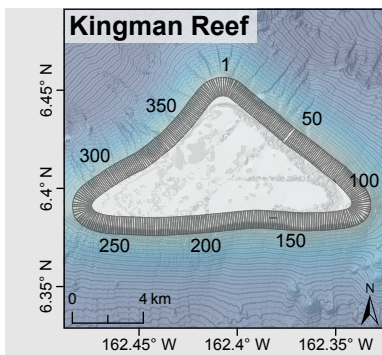
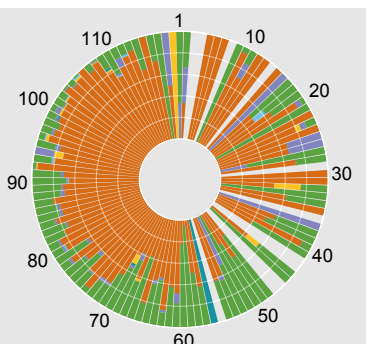
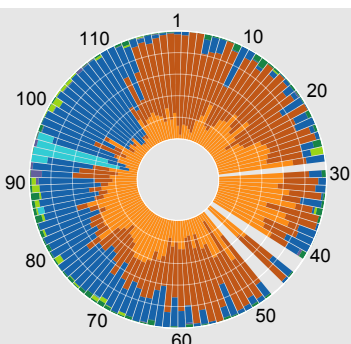
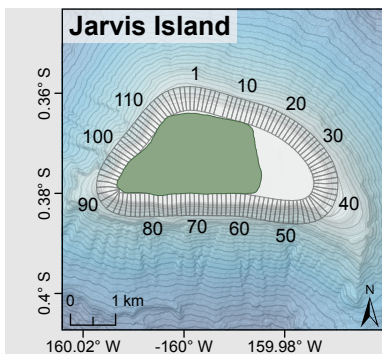
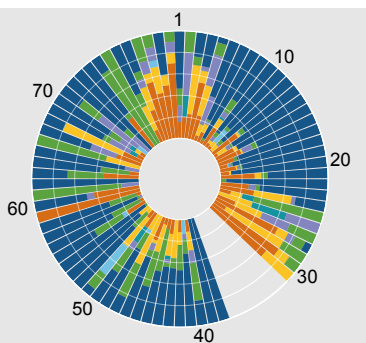
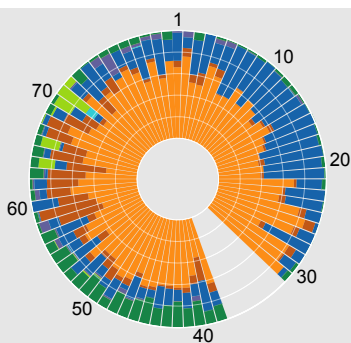
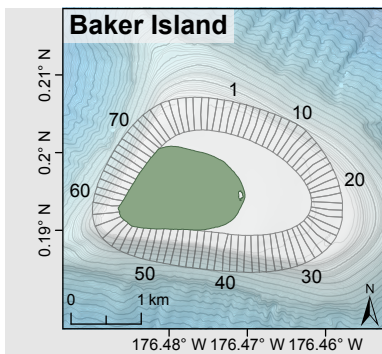
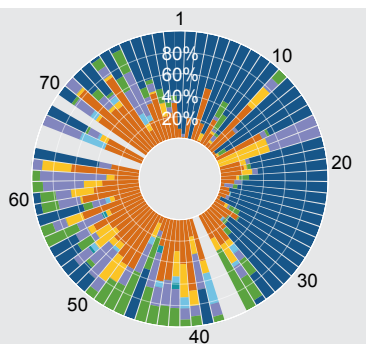
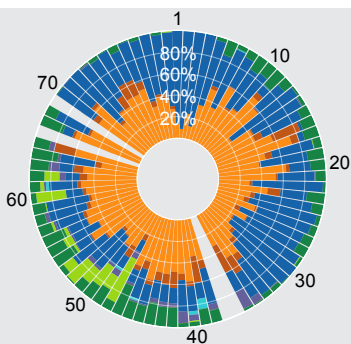
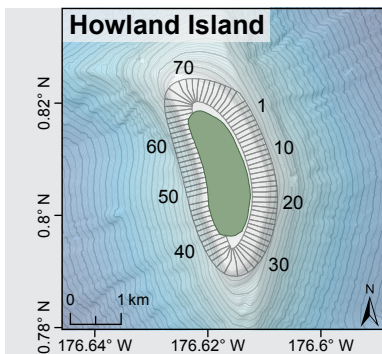
633

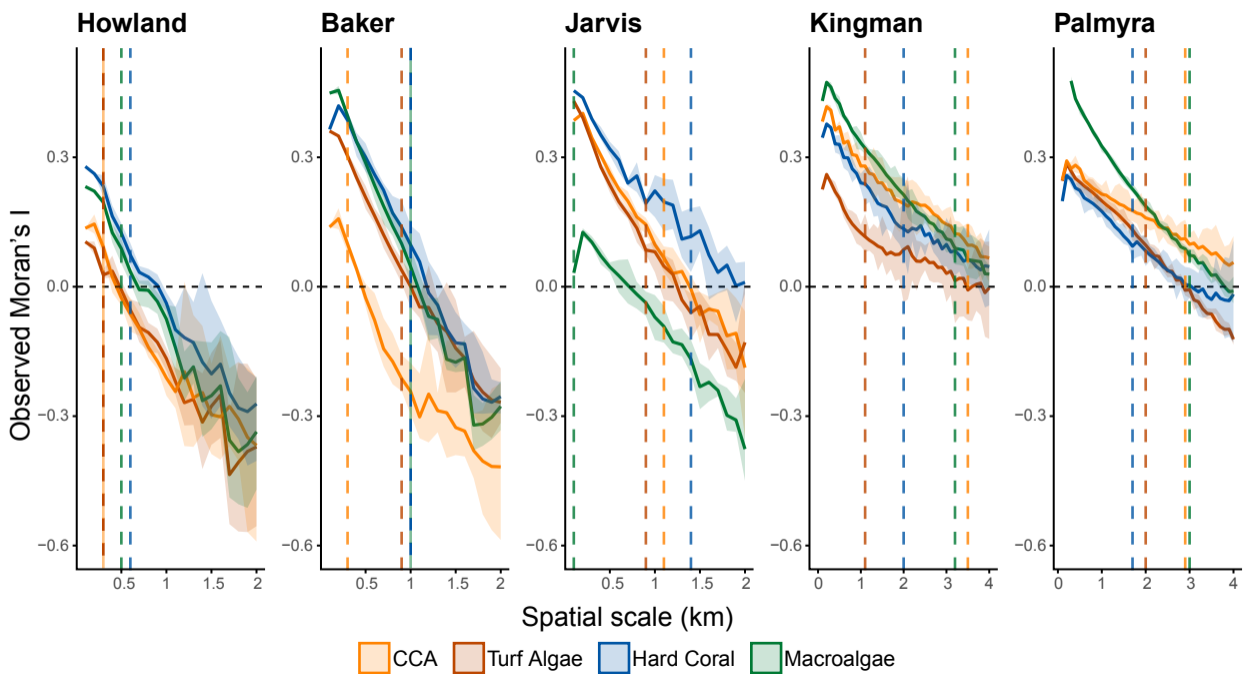
634

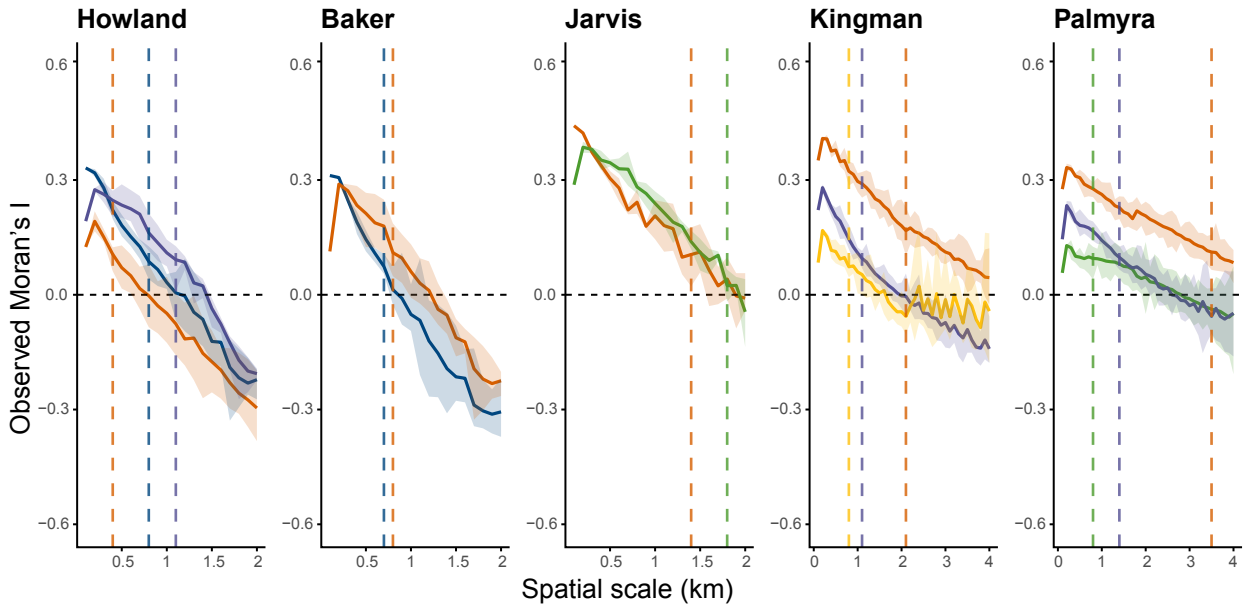
Island

Functional Group

Hard Coral Morphology







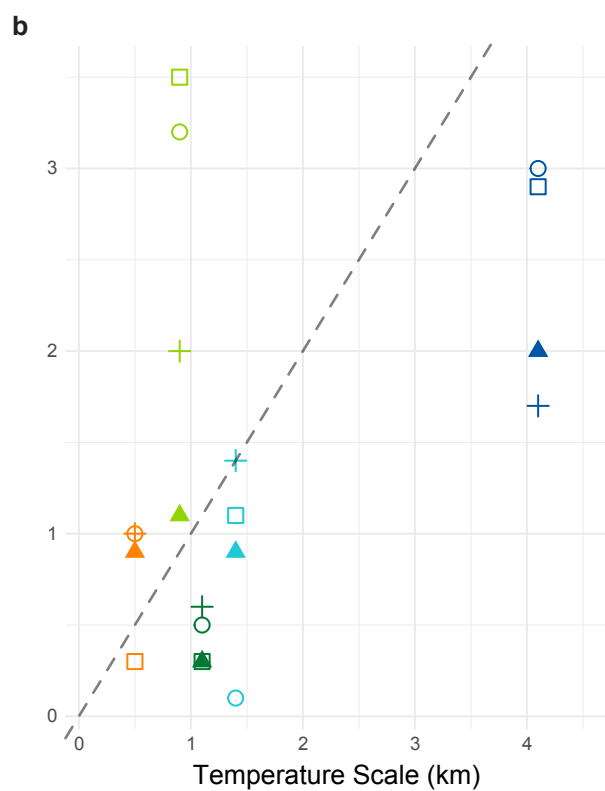
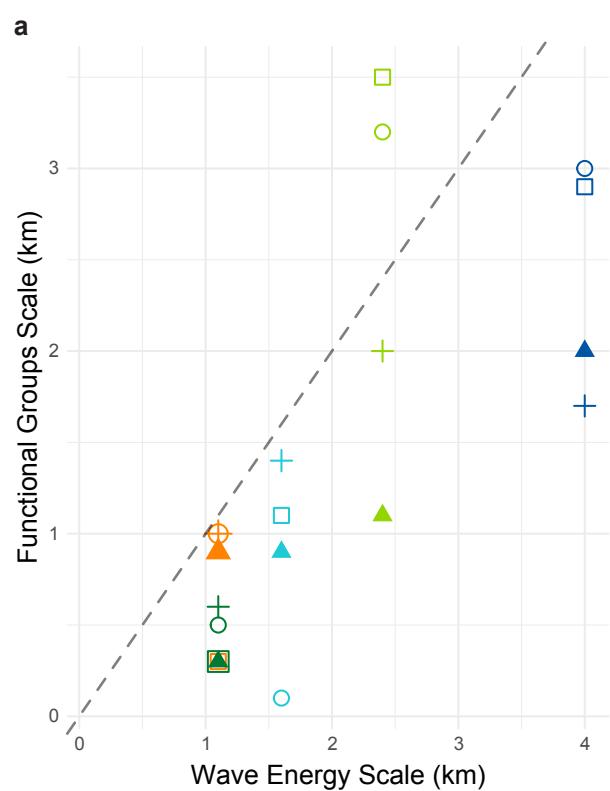
Branching

Submassive

Corymbose

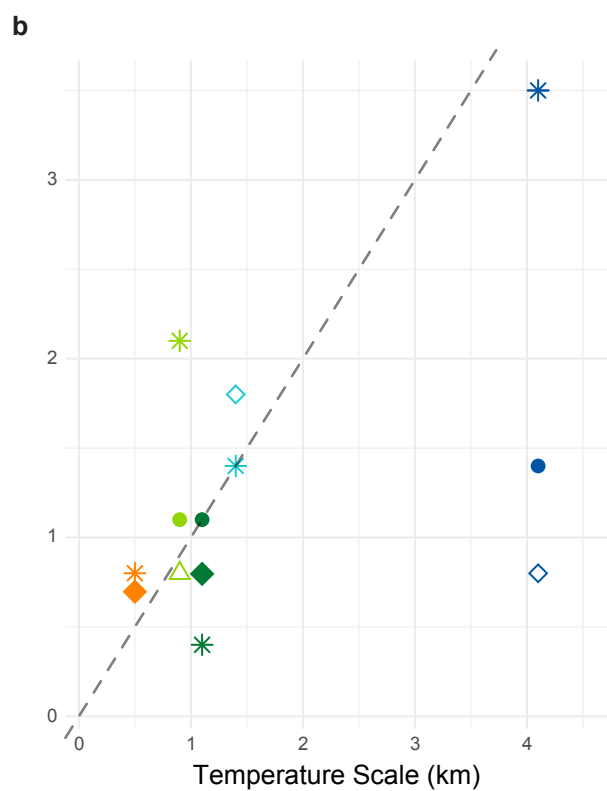
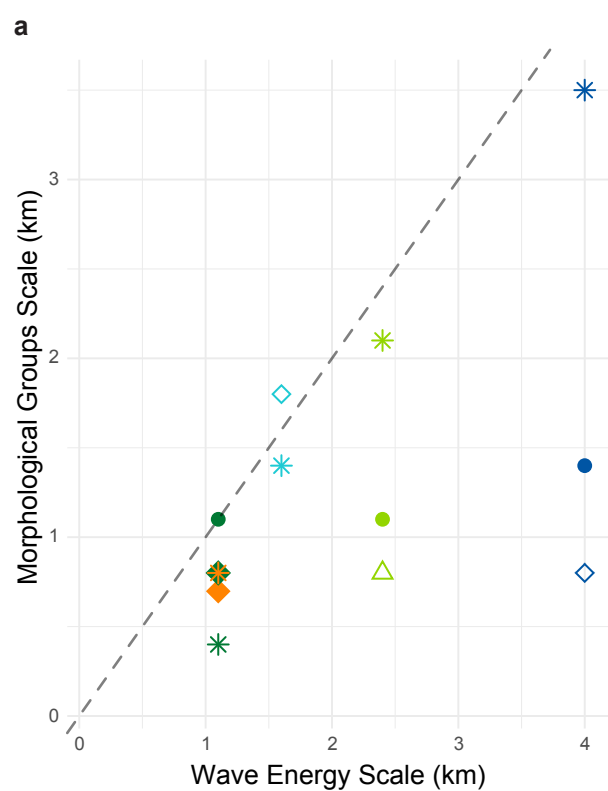
Encrusting

Plating



Island ■ Howland ■ Baker ■ Jarvis ■ Kingman ■ Palmyra

Functional Group □ CCA + Hard coral ○ Macroalgae ▲ Turf



Island Howland Baker Jarvis Kingman Palmyra

Morphology Branching Submassive Corymbose Encrusting Plating

Supplementary Material: Appendix 1

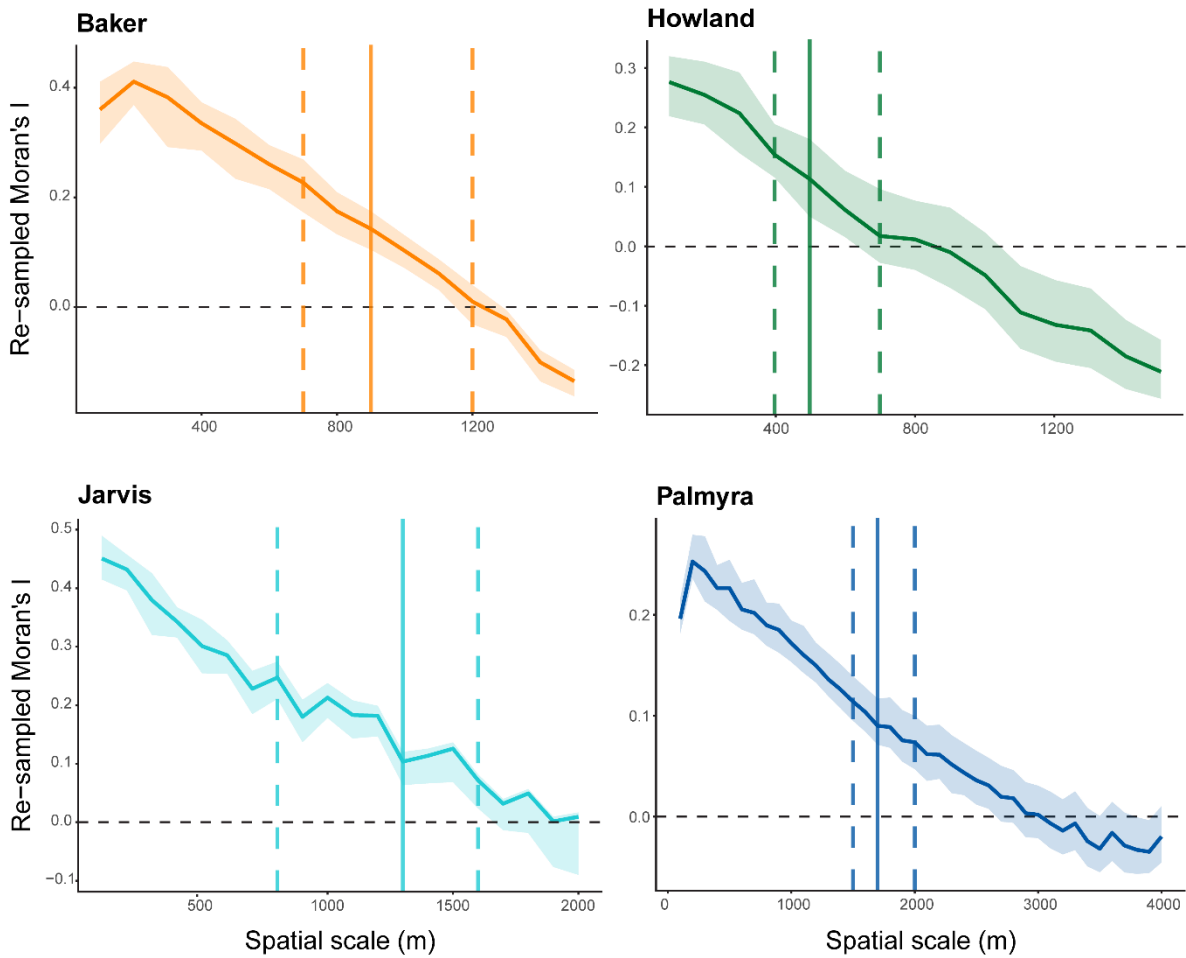


Figure A1. Sensitivity of Moran's I analysis to the number of island grid cells containing 'no data' (NA). The Moran's I analysis for hard coral percentage cover data was run 100 times with the same proportion of NA grid cells as Kingman (the island with the highest proportion of NA grid cells). NA grid cells were randomly distributed around the island each time the analysis was run. The result is a re-sampled Observed Moran's I (OMI) value across 100-m increment scales (solid coloured line) and the range in scale at which the OMI value is not significantly different from random ($p \geq 0.05$) (vertical dotted lines) and the mean scale across all 100 iterations (vertical solid line).

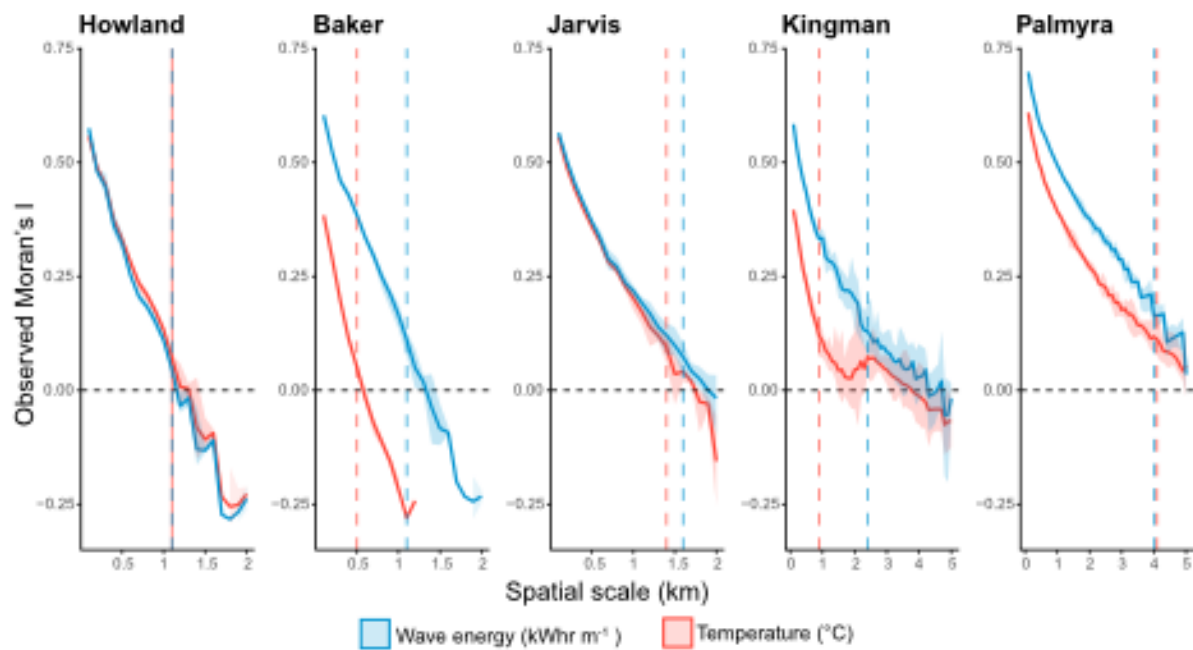

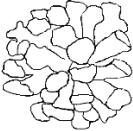





Figure A2. Patterns of spatial autocorrelation (solid coloured line) in surface wave energy (kW hr m⁻¹) and subsurface temperature (°C) at 100-m scale increments around five uninhabited central Pacific islands. The Observed Moran's I (OMI) value indicates a clustered distribution (+ve values), random distribution (0 value, horizontal dotted line) to increasingly dispersed (-ve values). The OMI is calculated for all possible starting points around each island and the range in these values for each scale is shown as the shaded region. The vertical dotted line shows the scale at which the OMI value is not significantly different from random for each benthic group ($p \geq 0.05$).

Table A1. Benthic functional group definitions used during our benthic identification process and their source.

Functional Groups	Description	Based on source:
Hard Coral	All Scleractinia	(Veron 2000)
CCA	Coraline Crustose Algae. Includes substrate and rubble covered in CCA. Also includes <i>Peyssonnelia</i> spp. which are functionally similar.	(Based on NOAA’s PIFSC benthic image analysis classification scheme)
Turf Algae	Mixture of short often indistinguishable Algae. Including the “epilithic algal matrix” and defined as a mixed community of filamentous algae and cyanobacteria generally < 2 cm tall Often appearing as fuzzy carpets. On hard surfaces, as well as rubble and sand.	(Based on NOAA’s PIFSC benthic image analysis classification scheme)
Macroalgae	Macroalgae or “fleshy” algae that are visible to the naked eye (typically >2cm) with evident structure and do not form crusts that adhere to rubble or substrate.	(Based on NOAA’s PIFSC benthic image analysis classification scheme)
Soft Coral	All Alcyonacea	(Fabricius et al. 2001)
Other Invertebrates	Includes Anenomes, Echinoderms, Fire coral, Holothurians and other invertebrates that are not included in other categories.	(Williams et al. 2013)
Soft Substrate	Soft substrate is sand which is unconsolidated sediment ranging in texture and size from fine to coarse. Assigned to areas clearly distinguished as sand generally >1cm deep and without anything clearly growing on top.	(Based on NOAA’s PIFSC benthic image analysis classification scheme)

Table A2. Descriptions for each hard coral morphology within our benthic images and the source. Drawings by HVF.

Hard Coral Morphology	Description	Based on source:	Grouping for this study
Branching 	Corals that branch and have secondary branches.	(Veron 2000)	Branching
Corymbose 	Corals with a bush-like structure and closely arranged branches.		Corymbose
Digitate 	Corals with finger-like upward projection. Grouped with corymbose as would have a similar level of vulnerability to wave action.	(Veron 2000)	Corymbose
Submassive 	Often an encrusting coral with irregular projections, or a short columnar appearance. Does not have similar size in all dimensions unlike massive corals.		Submassive
Columnar 	Corals with vertical projections or forming columns. The projections take up more space vertically than horizontally. Grouped with Submassive as have similar structure and level of vulnerability to wave action.	(Veron 2000)	Submassive
Massive		(Veron 2000)	Massive


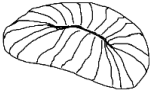
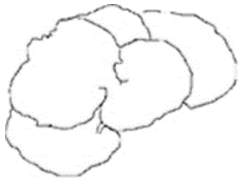

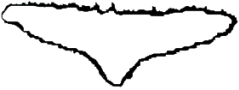

	<p>Boulder-like or dome shaped corals with similar shape in all dimensions.</p>		
<p>Free-living</p> 	<p>Corals that live unattached from the substrate. Often disk-shaped with a central mouth.</p>	<p>(Swanson et al. 2018)</p>	<p>Free-living</p>
<p>Plating</p> 	<p>The colony forms a plate-like structure that lifts off the surface of the substrate.</p>	<p>(Swanson et al. 2018)</p>	<p>Plating</p>
<p>Foliose</p> 	<p>Upright plates, often in whorls. Grouped with plating due to similarities in structure.</p>	<p>(Swanson et al. 2018)</p>	<p>Plating</p>
<p>Tabular</p> 	<p>Corals with a table like structure, with fused branches. May have had a central stalk attached to the substrate but this may be unseen by the angle of photos. If the coral is partly encrusting, classify as tabular. In this study, grouped together with Plating due to similarities in structure.</p>	<p>(Swanson et al. 2018)</p>	<p>Plating</p>
<p>Encrusting</p> 	<p>Vast majority of the coral adhered closely to the surface if not fully. Allowed for a one or two small abnormalities or projections. However, if numerous fragile projections were present, classified as submassive.</p>	<p>(Swanson et al. 2018)</p>	<p>Encrusting</p>

Table A3. Number of grid cells with 4 or more photos, compared to the total and as a percentage for each island.

Island	Grid cells with ≥ 4 photos	Total grid cells	Percentage of grid cells with ≥ 4 photos
Jarvis	114	119	95.8
Palmyra	340	394	86.3
Kingman	299	380	78.7
Baker	76	82	92.7
Howland	77	83	92.8